

Elimination of the Stark shift from the vibrational transition frequency of optically trapped $^{174}\text{Yb}^6\text{Li}$ molecules

Masatoshi Kajita*

National Institute of Information and Communications Technology, Koganei, Tokyo 184-8795, Japan

Geetha Gopakumar, Minori Abe, and Masahiko Hada

Department of Chemistry, Tokyo Metropolitan University, Minami-Osawa, Hachioji, Tokyo 192-0397, Japan

(Received 14 June 2011; published 10 August 2011)

Transition frequencies of cold molecules must be accurately evaluated to test the variance in the proton-to-electron mass ratio. Measuring the $X^2\Sigma(v,N) = (0,0) \rightarrow (1,0)$ transition frequency of optically trapped $^{174}\text{Yb}^6\text{Li}$ molecules is a promising method for achieving this goal. The Stark shifts induced by trap and probe (for the Raman transition) lasers are eliminated by choosing appropriate frequencies (magic frequencies) during the construction of the optical lattice. In the far-off resonance region, the Stark shift is found to be less than 10^{-16} even when the laser frequencies are detuned from the magic frequencies by ~ 1 MHz.

DOI: [10.1103/PhysRevA.84.022507](https://doi.org/10.1103/PhysRevA.84.022507)

PACS number(s): 33.20.-t, 37.10.Pq, 92.60.-e, 07.57.-c

I. INTRODUCTION

Precise measurements of molecular transitions are useful for testing the variance in the proton-to-electron mass ratio m_p/m_e because of their high sensitivities to m_p/m_e . For example, the pure vibrational and rotational transition frequencies are proportional to $(m_p/m_e)^{-1/2}$ and $(m_p/m_e)^{-1}$, respectively. The variances in m_p/m_e were first discussed on the basis of astronomical measurements, for which the variance over billions of years can be detected [1–4]. The current estimated upper limit in astronomical measurement is $[d(m_p/m_e)/dt]/(m_p/m_e) = 1.9 \times 10^{-16}/\text{yr}$ [4].

In astronomical research, we cannot distinguish between space and time variances. To test for the pure time variances in m_p/m_e , one must compare the measurements of the molecular transitions with those of the atomic transition frequencies, such as $^1\text{S}_0$ - $^3\text{P}_0$ transition frequencies of the ^{87}Sr atom [5] or $^{27}\text{Al}^+$ ion [6], in the laboratory. Shelkovich *et al.* measured the vibrational transition frequency of SF_6 molecules in a thermal beam at an uncertainty level of 10^{-14} using a Cs fountain clock as a reference and obtained $[d(m_p/m_e)/dt]/(m_p/m_e)$ to be $(-3.8 \pm 5.6) \times 10^{-14}/\text{yr}$ [7].

Several authors have proposed measuring the transition frequencies of cold molecules, which have greater sensitivities than pure vibrational or rotational transition frequencies. Bethlem *et al.* suggested measuring the NH_3 inversion transition frequency f_{inv} , with which the variance in (m_p/m_e) with the order of $\Delta(m_p/m_e)/(m_p/m_e) \approx 10^{-15}$ is detected as the variance in f_{inv} with the order of $\Delta f_{\text{inv}}/f_{\text{inv}} \approx 4.2 \times 10^{-15}$ [8]. However, it is not easy to obtain the uncertainty of f_{inv} below 10^{-14} , because a measurement time longer than 150 h and a magnetic field lower than 1 mG are required. Frambaum *et al.* and DeMille *et al.* suggested measuring the transition between the vibrational excited state and the fine-structure excited state, which are quasidegenerated [9,10]. The transition frequency f_d is given by the difference between the vibrational transition frequency f_{vib} [$\propto(m_p/m_e)^{-1/2}$] and the fine-structure transition frequency f_{FS} [no dependence on (m_p/m_e)].

Then the sensitivity of f_d on the variance in (m_p/m_e) is given by $\Delta f_d/f_d = (f_{\text{vib}}/f_d)/2 \times \Delta(m_p/m_e)/(m_p/m_e)$, while $\Delta f_{\text{vib}}/f_{\text{vib}} = \Delta(m_p/m_e)/(m_p/m_e)/2$. We must also consider the frequency uncertainty, which is limited by the shift induced by Stark or Zeeman effects. Using the frequency shifts of f_{vib} and f_{FS} , δf_{vib} and δf_{FS} , the frequency uncertainty of f_d is given by $|\delta f_d|/f_d = |\delta f_{\text{vib}} - \delta f_{\text{FS}}|/f_d$. When $(\Delta f_d/\delta f_d)$ and $(\Delta f_{\text{vib}}/\delta f_{\text{vib}})$ are compared, it is more advantageous to measure f_{vib} when $|\delta f_{\text{vib}} - \delta f_{\text{FS}}| > |\delta f_{\text{vib}}|$.

We proposed using other methods to measure pure vibrational transition frequencies with an uncertainty lower than 10^{-15} . At first, we proposed measuring the vibrational transition frequencies of ^{40}CaH , ^{24}MgH , or ^9BeH molecules [11,12], which are buffer gas cooled and loaded in the magnetic trap [13]. After that, we proposed measuring the pure vibrational transition frequencies of XH^+ ($X = ^{24}\text{Mg}$, ^{40}Ca , ^{88}Sr , ^{138}Ba , ^{64}Zn , ^{114}Cd , ^{174}Yb , and ^{202}Hg) molecular ions [14,15].

In our previous work, the frequency shifts induced by the trap (electric or magnetic) field and probe laser limited the frequency accuracies attainable. Molecules in the optical lattice are advantageous for measuring a transition frequency with a low frequency uncertainty because (1) the molecules and probe laser interact for a long time, (2) molecules are localized within the Lamb-Dicke region, (3) the measurement is performed with a large number of molecules, and (4) the method suppresses the collisional shift (in two- or three-dimensional lattices). The Stark shift induced by the trap laser is eliminated by using the trap laser frequency (magic trap frequency) at which the Stark shift in the upper and lower states are equal. The $^1\text{S}_0$ - $^3\text{P}_0$ transition frequency of the Sr atom in an optical lattice was measured with an uncertainty of less than 10^{-16} with this method [5].

Zelevinski *et al.* suggested measuring the $X^1\Sigma, v = 27 \rightarrow -3$ transition frequency of $^{88}\text{Sr}_2$ molecules in an optical lattice ($v = \text{vibrational quantum number}$), whose sensitivity to (m_p/m_e) is higher than that for the $v = 0 \rightarrow 1$ transition [16]. Kotochigova *et al.* demonstrated the existence of magic trap frequencies in the quasidegenerated regions that have transitions from the $v = 27$ or -3 states [17]. However, note that the

*kajita@nict.go.jp

Stark shift of the transition frequency is sensitive to slight fluctuations in the trap laser frequency in the quasiresonant region. Therefore, the trap laser frequency must be locked to the magic trap frequency with a very high stability (<1 kHz). For $^{88}\text{Sr}_2$ molecules, magic trap frequencies do not exist in the far-off resonance region (see Sec. II).

This paper discusses the possibility of eliminating the Stark shift in the $^{174}\text{Yb}^6\text{Li}$ $X^2\Sigma(v, N) = (0, 0) \rightarrow (1, 0)$ transition frequency $f_c (=4.17 \text{ THz}$ [18]) induced by the trap laser. Here, N denotes the rotational quantum number. For the $^{174}\text{Yb}^6\text{Li}$ vibrational transition frequency, a magic trap frequency also exists in the far-off resonance region. For the magic trap frequency in the far-off resonance region, the Stark shift is less than 10^{-16} if the trap laser frequency is detuned from the magic trap frequency by $\sim 1 \text{ MHz}$. The $(0, 0) \rightarrow (1, 0)$ transition can be observed using a Raman transition. For the Raman transition, two probe lasers are used, which have a frequency difference fixed to f_c . Also, the Stark shift induced by the Raman lasers can be eliminated by using the special Raman laser frequencies (magic Raman frequency). Although the elimination of the Stark shift induced by the Raman lasers was previously proposed for the $^{88}\text{Sr}^1\text{S}_0\text{-}^3\text{P}_0$ transition [19], this is the first proposal to measure the molecular vibrational frequencies by using the magic trap and Raman frequencies in the far-off resonance region. The Stark shifts were estimated by using the values of transition frequencies and dipole moments, obtained via an *ab initio* calculation [18].

II. OPTICAL TRAP AND STARK SHIFT INDUCED BY THE TRAPPED LASER LIGHT

When a laser light (power density I_T , frequency f_T) irradiates molecules in the i th state, the electric field is given by $\sqrt{2I_T/\epsilon_0 c} \cos(2\pi f_T t)$ and the second-order Stark energy shift is given by

$$\epsilon_S(i) = S_i(f_T) \frac{I_T}{\epsilon_0 c},$$

$$S_i(f_T) = \frac{1}{2} \sum_{k \neq i} \left[\frac{|\mu_{ik}|^2}{E_i - E_k - hf_T} + \frac{|\mu_{ik}|^2}{E_i - E_k + hf_T} \right], \quad (1)$$

where μ_{ik} is the dipole matrix element between the i and the k states, $E_{i,k}$ are the energies of the respective states, and $S_i(f_T)$ is the second-order Stark coefficient.

In this paper, we discuss the Stark shift of the $X^2\Sigma(v, N) = (0, 0) \rightarrow (1, 0)$ transition frequency f_c . When f_T is much higher than the vibrational frequencies, the second-order Stark coefficients of the $X^2\Sigma(v, N) = (0, 0)$ and $(1, 0)$ states (denoted S_0 and S_1 , respectively) are dominated by the terms of interactions with different electronic states $\Phi (=A^2\Sigma, B^2\Sigma, C^2\Sigma, A^2\Pi, B^2\Pi, C^2\Pi)$. S_0 and S_1 are given by

$$S_0(f_T) = - \sum_{\Phi, v} \frac{\mu_0(\Phi, v)^2}{3h} \frac{f_e(\Phi, v)}{f_e(\Phi, v)^2 - f_T^2},$$

$$S_1(f_T) = - \sum_{\Phi, v} \frac{\mu_1(\Phi, v)^2}{3h} \frac{f_e(\Phi, v) - f_c}{[f_e(\Phi, v) - f_c]^2 - f_T^2}, \quad (2)$$

where $\mu_j(\Phi, v)$ is the $X^2\Sigma(v = j) - \Phi(v)$ ($j = 0, 1$) transition dipole moment. The $N = 0$ states only have dipole couplings with $N = 1$ states. The $X^2\Sigma(v = j, N = 0) - \Phi(v, N = 1)$ transition dipole matrix elements are $\mu_j(\Phi, v)/\sqrt{3}$ and are independent of the photon polarization [17]. The $f_e(\Phi, v)$ is the $X^2\Sigma(v, N) = (0, 0) \rightarrow \Phi(v, 1)$ transition frequency. Values of $\mu_0(\text{table}\Phi, v)$ and $\mu_1(\Phi, v)$ are listed in Table I and those of $f_e(\Phi, v)$ are listed in Table II [18].

The second-order Stark shift in the $^{174}\text{Yb}^6\text{Li}$ $X^2\Sigma(v, N) = (0, 0) \rightarrow (1, 0)$ transition frequency is given by

$$\delta f_L = \frac{[S_1(f_T) - S_0(f_T)] I_T}{h \epsilon_0 c}. \quad (3)$$

If the condition $S_1 - S_0 = 0$ is satisfied by the trap laser frequency (magic trap frequency), the second-order Stark shift in the transition frequency can be eliminated. To find the solutions for the magic trap frequencies, δf_L was calculated as a function of the trap laser frequency f_T , taking the trap laser power density to be 23 kW/cm^2 . The result is shown in Fig. 1 for the range spanning from 270 THz (1.11 μm) to 420 THz (714 nm).

The quasiresonant regions have many solutions for the magic trap frequencies, as shown in the work by Kotochigova *et al.* [17]. However, the magic trap frequencies in the $X^2\Sigma - A^2\Sigma$ quasiresonant region are not useful for experimental purposes, because $|\delta f_L/f_c|$ is larger than 10^{-14} when f_T is detuned from the magic trap frequencies by $\sim 100 \text{ kHz}$ ($|d(\delta f_L/f_c)/df_T| > 10^{-13}/\text{MHz}$). To use the magic trap frequencies in the $X^2\Sigma - A^2\Sigma$ quasiresonant region, the trap laser frequency must be stabilized using a high-finesse reference cavity.

Note that the rate of the electronic transitions induced by the trap laser limits the possible measurement time and

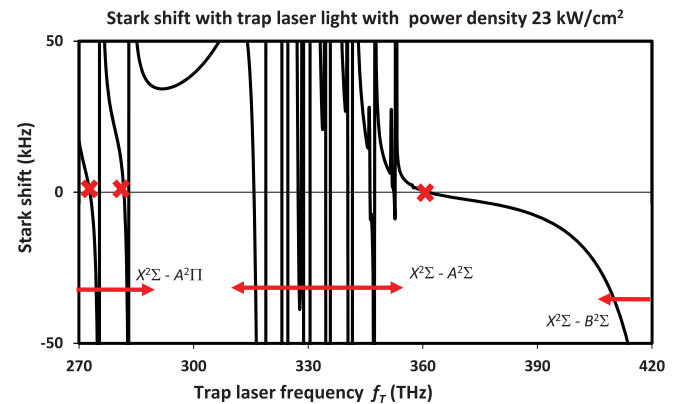


FIG. 1. (Color online) Dependence of the Stark shift of the $^{174}\text{Yb}^6\text{Li}$ $X^2\Sigma(v, N) = (0, 0) \rightarrow (1, 0)$ transition frequency on the trap laser frequency. It is assumed that the laser power density is 23 kW/cm^2 . The magic trap frequencies, listed in Table III, are highlighted [(red crosses)]. The red arrows denote the frequency region that is quasiresonant with the $X^2\Sigma - A^2\Pi$, $A^2\Sigma$, and $B^2\Sigma$ transitions.

TABLE I. Transition dipole moments between the $^{174}\text{Yb}^6\text{Li}$ $X^2\Sigma(v=0 \text{ and } 1) - \Phi(v)$ states $\mu_0(\Phi, v)$ and $\mu_1(\Phi, v)(v=0) - 6$ [18]. $\mu_0(A^2\Pi, v)$ and $\mu_1(A^2\Pi, v)$ are shown for higher values of v (shown in parentheses), because the $X^2\Sigma - A^2\Pi$ coupling is not diagonal. Only a rough estimate is given for the $\Phi = C^2\Sigma$ and $C^2\Pi$ states.

	$v=0$	$v=1$	$v=2$	$v=3$	$v=4$	$v=5$	$v=6$
$\mu_0(A^2\Sigma, v)$ (D)	4.256	0.900	0.419	0.164	0.070	0.027	0.011
$\mu_1(A^2\Sigma, v)$ (D)	1.732	3.459	1.394	0.814	0.406	0.201	0.092
$\mu_0(B^2\Sigma, v)$ (D)	8.160	0.719	1.329	0.171	0.304	0.145	0.003
$\mu_1(B^2\Sigma, v)$ (D)	1.151	7.399	3.460	1.068	0.011	0.511	0.150
$\mu_0(C^2\Sigma, v)$ (D)	4.380	0.000	0.000	0.000	0.000	0.000	0.000
$\mu_1(C^2\Sigma, v)$ (D)	0.000	4.380	0.000	0.000	0.000	0.000	0.000
$\mu_0(A^2\Pi, v)$ (D)	0.137(4)	0.186(5)	0.229(6)	0.259(7)	0.272(8)	0.264(9)	0.241(10)
$\mu_1(A^2\Pi, v)$ (D)	0.121(3)	0.144(4)	0.139(5)	0.272(10)	0.327(11)	0.346(12)	0.335(13)
$\mu_0(B^2\Pi, v)$ (D)	0.663	1.028	1.204	1.221	1.132	0.989	0.834
$\mu_1(B^2\Pi, v)$ (D)	1.152	1.231	0.856	0.328	0.152	0.492	0.687
$\mu_0(C^2\Pi, v)$ (D)	6.365	0.000	0.000	0.000	0.000	0.000	0.000
$\mu_1(C^2\Pi, v)$ (D)	0.000	6.365	0.000	0.000	0.000	0.000	0.000

the minimum spectrum linewidth. The minimum linewidth is given by

$$\frac{\gamma}{2\pi} = \frac{1}{4\pi} \frac{I_T}{\epsilon_0 c} \sum_{\Phi, v} \left[\frac{\Gamma(\Phi, v) \mu_0(\Phi, v)^2}{h^2 [f_e(\Phi, v) - f_T]^2} + \frac{\Gamma(\Phi, v) \mu_1(\Phi, v)^2}{h^2 [f_e(\Phi, v) - f_c - f_T]^2} \right], \quad (4)$$

where $\Gamma(\Phi, v)$ denotes the spontaneous scattering rate in the (Φ, v) state. Values of $\Gamma(\Phi, 0)$ are listed in Table II. In the $X^2\Sigma - A^2\Sigma$ quasiresonant region, $\gamma/2\pi > 10$ Hz.

Table III lists three solutions for the magic trap frequencies: 272.99 THz (1.097 μm), 281.76 THz (1.064 μm), and 361.43 THz (830 nm). With these magic trap frequencies, the conditions $|d(\delta f_L/f_c)/df_T| < 10^{-14}/\text{MHz}$ and $\gamma/2\pi < 1$ Hz are also simultaneously satisfied when the trap laser power density is high enough for the potential depth to be larger than 10 μK . These magic trap frequencies will hopefully be used in measurements, because the frequencies of a Ti-sapphire (fiber) laser can be locked within 100(10) kHz using a reference cavity with a simple structure. The magic trap frequencies at 272.99 and 281.76 THz are in the $X^2\Sigma - A^2\Pi$ quasiresonant region. For both these magic trap frequencies, $|d(\delta f_L/f_c)/df_T|$ and $\gamma/2\pi$ are much smaller than those in the $X^2\Sigma - A^2\Sigma$ quasiresonant region because of the small values of $\mu_0(A^2\Pi, v)$ and $\mu_1(A^2\Pi, v)$. However, the potential depth is large enough because of the strong $X^2\Sigma - A^2\Sigma$ and $X^2\Sigma - B^2\Sigma$ couplings.

The magic trap frequency at 361.43 THz is in the far-off resonance region (separated by more than 10 THz from transitions with $\mu_0(\Phi, v)$, $\mu_1(\Phi, v) > 0.1$ D). For this magic trap frequency, $|\delta f_L/f_c| < 10^{-16}$ when f_T is detuned from this magic trap frequencies by ~ 1 MHz. Here we discuss δf_L in the far-off resonance frequency region between 350 and 420 THz using a simplified model, which takes only the $X^2\Sigma - A^2\Sigma$ and $X^2\Sigma - B^2\Sigma$ couplings into account. Table I shows that both couplings are almost diagonal. In the far-off resonance region, $|f_v(\Phi) - f_c| \ll |f_e(\Phi, 0) - f_T|$ is satisfied, where $f_v(\Phi) [=f_e(\Phi, 1) - f_e(\Phi, 0)]$ is the $\Phi(v, N) = (0, 1) \rightarrow (1, 1)$ transition frequency. The second-order Stark coefficient for the $(0, 0) \rightarrow (1, 0)$ transition frequency is approximately given by

$$S_1(f_T) - S_0(f_T) \approx \frac{\mu_0(A^2\Sigma, 0)^2}{6h} \frac{f_v(A^2\Sigma) - f_c}{[f_e(A^2\Sigma, 0) - f_T]^2} + \frac{\mu_0(B^2\Sigma, 0)^2}{6h} \frac{f_v(B^2\Sigma) - f_c}{[f_e(A^2\Sigma, 0) - f_T]^2}. \quad (5)$$

Because $f_v(A^2\Sigma) > f_c > f_v(B^2\Sigma)$, the first (second) term in Eq. (5) is positive (negative). For an appropriate value of f_T (magic trap frequency), the two terms in Eq. (5) cancel each other out. The magic trap frequency given by Eq. (5) is 3 THz higher than that given by detailed calculation. For a Sr_2 molecule, the vibrational frequency in the ground state is the lowest among all electronic states, and the Stark shift in the vibrational transition frequency is always positive, except

TABLE II. The $X^2\Sigma(v=0, N=0) \rightarrow \Phi(v, N=1)$ transition frequencies $f_e(\Phi, v)(v=0, 1, 2)$, the $\Phi(v, N) = (0, 1) \rightarrow (1, 1)$ transition frequency $f_v(\Phi)$, and the spontaneous emission rate from the $(\Phi, 0)$ states $\Gamma(\Phi, 0)$ for a $^{174}\text{Yb}^6\text{Li}$ molecule [18].

	$f_e(\Phi, 0)$ (THz)	$f_e(\Phi, 1)$ (THz)	$f_e(\Phi, 2)$ (THz)	$f_v(\Phi)$ (THz)	$\Gamma(\Phi, 0)$ (s^{-1})
$A^2\Sigma$	323.2	328.9	334.6	6.02	7.0×10^6
$B^2\Sigma$	442.9	445.6	448.7	3.19	6.9×10^7
$C^2\Sigma$	561.1	572.8	584.4	11.6	3.9×10^7
$A^2\Pi$	177.2	186.4	195.5	8.95	1.6×10^4
$B^2\Pi$	431.3	439.0	446.5	8.00	1.2×10^7
$C^2\Pi$	754.7	761.7	768.7	6.99	2.1×10^8

TABLE III. Trap laser frequencies f_T , where the Stark shift in the $^{174}\text{Yb}^6\text{Li } X^2\Sigma(v, N) = (0, 0) \rightarrow (1, 0)$ transition frequency ($\delta f_L/f_c$) is 0 (this is known as the magic trap frequency). Also listed the slope of the Stark shift versus the trap laser frequency $|d(\delta f_L/f_c)/df_T|$, the potential depth, and the minimum linewidth $\gamma/2\pi$ limited by photon scattering, when the power density of the trap laser is 23 kW/cm^2 . Only magic trap frequencies in which the following conditions are simultaneously satisfied are listed: $|d(\delta f_L/f_c)/df_T| < 3 \times 10^{-15}/\text{MHz}$, the potential depth is larger than $10 \mu\text{K}$, and the minimum linewidth is narrower than 1 Hz .

f_T (THz)	$d(\delta f_L/f_c)/df_T$ (/MHz)	Potential depth (μK)	$\gamma/2\pi$ (Hz)
272.99	-1.8×10^{-15}	20.0	0.06
281.76	-5.4×10^{-15}	22.3	0.06
361.43	-8.0×10^{-17}	13.7	0.27

in the quasiresonant regions [17,20]. Therefore, there is no solution for the magic trap frequency in the far-off resonance region for a Sr_2 molecule.

Here we estimate the influence of the fourth-order Stark shift, which is the remaining Stark shift when the second-order Stark shift is 0. The fourth-order Stark energy shift $\epsilon_Q(i)$ is estimated by rewriting Eq. (1) as

$$\epsilon_S(i) + \epsilon_Q(i) = \frac{I_T}{2\epsilon_0 c} \sum_{k \neq i} \left[\frac{|\mu_{ik}|^2}{E_i - E_k - hf_T + \epsilon_S(i) - \epsilon_S(k)} + \frac{|\mu_{ik}|^2}{E_i - E_k + hf_T + \epsilon_S(i) - \epsilon_S(k)} \right],$$

$$\epsilon_Q(i) = \frac{I_T}{2\epsilon_0 c} \sum_{k \neq i} [\epsilon_S(i) - \epsilon_S(k)] \left[\frac{|\mu_{ik}|^2}{(E_i - E_k - hf_T)^2} + \frac{|\mu_{ik}|^2}{(E_i - E_k + hf_T)^2} \right]. \quad (6)$$

Considering $[E_i - E_k \pm hf_T]/h > 30 \text{ THz}$ and $|\mu_{ik}| \sqrt{2I_T/\epsilon_0 c}/h < 1 \text{ GHz}$, $\epsilon_Q(i)/h$ is less than 0.03 mHz and the influence of the fourth-order Stark shift is less than 10^{-17} .

III. STARK SHIFT INDUCED BY RAMAN LASERS

The $X^2\Sigma(v, N) = (0, 0) \rightarrow (1, 0)$ transition frequency can be measured by probing the two-photon Raman transition using two lasers (power densities I_{R0} , I_{R1} and frequencies f_{R0} , f_{R1} , where $f_{R1} = f_{R0} - f_c$). In this case, the Rabi frequency $\Omega_R/2\pi$ is given by

$$\frac{\Omega_R(I_{R0}, I_{R1}, f_{R0})}{2\pi} = \frac{\sqrt{I_{R0}I_{R1}}}{3\epsilon_0 ch^2} \sum_{\Phi, v} \frac{\mu_0(\Phi, v) \mu_1(\Phi, v)}{f_e(\Phi, v) - f_{R0}}, \quad (7)$$

and the Stark shift induced by the lasers for Raman transition is given by

$$\delta f_R = \delta f_{R0} + \delta f_{R1},$$

$$\delta f_{Rn} = \frac{[S_1(f_{Rn}) - S_0(f_{Rn})] I_{Rn}}{h \epsilon_0 c} \quad (n = 0, 1). \quad (8)$$

Figure 2 shows the Stark frequency shift δf_R , which was calculated as a function of the higher of the two Raman laser frequencies f_{R0} , taking $I_{R0} = I_{R1} = 0.6 \text{ W/cm}^2$. For Raman lasers, there are many solutions for frequencies where $\delta f_R = 0$ (magic Raman frequencies) in the quasiresonant region of the $X^2\Sigma \rightarrow A^2\Sigma$ transition. For Raman lasers with power densities of less than 1 W/cm^2 , the slope of $\delta f_R/f_c$ versus f_{R0} , $|d(\delta f_R/f_c)/df_{R0}|$, is less than 10^{17} MHz and $\gamma/2\pi$ is much less than 1 Hz in all the frequency regions. The Stark shift is

significant when the ratio of power densities of the two Raman lasers I_{R0}/I_{R1} fluctuates and δf_{R0} and δf_{R1} do not cancel each other out. For many magic Raman frequencies in the $X^2\Sigma - A^2\Sigma$ quasiresonant region, $|\delta f_R/f_c|$ is larger than 10^{-14} when the fluctuation of I_{R0}/I_{R1} is larger than 1% ($|\delta f_{R0}/f_c| > 10^{-12}$).

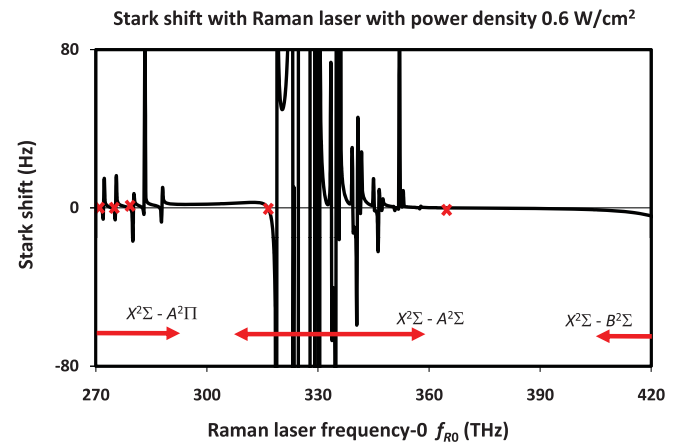


FIG. 2. (Color online) Dependence of the Stark shift of the $^{174}\text{Yb}^6\text{Li } X^2\Sigma(v, N) = (0, 0) \rightarrow (1, 0)$ transition frequency on the higher of the Raman laser frequencies f_{R0} (the other Raman laser frequency f_{R1} is $f_c = 4.17 \text{ THz}$ lower). It is assumed that the laser power densities of both lasers are 0.6 W/cm^2 . The magic Raman frequencies, listed in Table IV, are highlighted [(red) exes]. The (red) arrows denote the frequency region that is quasiresonant with the $X^2\Sigma - A^2\Pi$, $A^2\Sigma$, and $B^2\Sigma$ transitions.

TABLE IV. Magic Raman frequencies f_{R0} and f_{R1} ($= f_{R0} - f_c$) for which the Stark shift in the $^{174}\text{Yb}^6\text{Li } X^2\Sigma(v, N) = (0, 0) \rightarrow (1, 0)$ transition frequency ($\delta f_R/f_c$) is 0, when the power densities of two lasers are equal. The Stark shift with one laser $|\delta f_{R0,1}|/f_c$, the slope of the Stark shift versus the trap laser frequency $d(\delta f_R/f_c)/df_T$, and the Rabi frequency $\Omega_R/2\pi$ when the power densities of the two lasers are both 0.6 W/cm^2 are listed. Only magic Raman frequencies for which the Stark shift with one laser is less than 4×10^{-13} when the laser intensity is high enough to obtain $\Omega_R/2\pi > 1 \text{ Hz}$ are listed.

f_{R0} (THz)	f_{R1} (THz)	$ \delta f_{R0,1} /f_c$	$d(\delta f_R/f_c)/df_T$ (/MHz)	$\Omega_R/2\pi$ (Hz)
274.25	270.08	1.4×10^{-13}	-2.1×10^{-19}	5.9
278.76	274.59	1.6×10^{-13}	-3.2×10^{-18}	7.0
282.59	278.42	1.7×10^{-13}	-1.7×10^{-19}	7.0
316.55	312.38	3.3×10^{-13}	-8.0×10^{-19}	27.0
364.25	360.08	4.8×10^{-15}	-4.5×10^{-21}	1.1

Table IV lists the solutions for the magic Raman frequencies that are useful for experimental purposes. In these cases, the conditions $|\delta f_{R0,1}/f_c| < 4 \times 10^{-13}$ and $\Omega_R/2\pi > 1 \text{ Hz}$ are simultaneously satisfied with $I_{R0} = I_{R1} = 0.6 \text{ W/cm}^2$. The magic Raman frequency in the far-off resonance region (364.25 THz + 360.08 THz) is particularly advantageous for observing the Raman transition that eliminates the Stark shift because $|\delta f_R/f_c| < 10^{-16}$ when I_{R0}/I_{R1} varies between 0.98 and 1.02.

IV. OTHER FREQUENCY SHIFTS

In this section, we consider the frequency shifts induced by effects, except for the Stark shift induced by the trap and Raman lasers. The Stark shift induced by blackbody radiation is given by

$$\delta f_B = \int \frac{S_1(f) - S_0(f)}{h} \frac{8\pi h f^3}{\epsilon_0 c^3} \frac{1}{\exp(hf/k_B T_C) - 1} df, \quad (9)$$

where T_C is the surrounding temperature. When $T_C = 300$ (100) K, $\delta f_B/f_c = -6.1 \times 10^{-16}$ (-7.3×10^{-18}). When T_C is stabilized within $300 \pm 5 \text{ K}$, the uncertainty of $\delta f_B/f_c$ is 4×10^{-17} .

The Stark shift induced by the static electric field E_{dc} is given by

$$\delta f_{dc} = \left[\frac{\mu_0^2}{6hB_0} - \frac{\mu_1^2}{6hB_1} \right] E_{dc}^2 \quad (10)$$

where μ_0 (μ_1) and B_0 (B_1) denotes the permanent dipole moment and rotational constant in the $X^2\Sigma, v = 0$ ($v = 1$) state. Using the values $\mu_0 = 0.136 \text{ D}$, $\mu_1 = 0.139 \text{ D}$, $B_0 = 6.44 \text{ GHz}$, and $B_1 = 6.36 \text{ GHz}$ [18], $\delta f_{dc}/f_c E_{dc}^2 = -1.7 \times 10^{15} \text{ (V/cm)}^2$. Keeping $E_{dc} < 0.2 \text{ V/cm}$, $|\delta f_{dc}/f_c| < 10^{-16}$ is satisfied.

The Zeeman shift of the $X^2\Sigma(v, N, F, M) = (0, 0, 3/2, \pm 3/2) \rightarrow (1, 0, 3/2, \pm 3/2)$ transitions is estimated to be $\mp 5 \times 10^{-17}$ with a magnetic field of 1 G [21], where F is the quantum number of the hyperfine structure and M is the component of F parallel to the magnetic field. Note that the average of the $M = 3/2 \rightarrow 3/2$ and $M = -3/2 \rightarrow -3/2$ transition frequencies is free from the Zeeman shift.

The second-order Doppler shift and collision shift are lower than 10^{-19} , when the molecules with a kinetic energy lower than $10 \mu\text{K}$ are trapped in a two- or three-dimensional lattice.

V. CONCLUSION

In this paper, we explained how the $^{174}\text{Yb}^6\text{Li } X^2\Sigma(v, N) = (0, 0) \rightarrow (1, 0)$ transition frequency can be measured with an uncertainty of less than 10^{-16} by eliminating the frequency shifts induced by the trap field and the probe laser lights. The molecules are trapped via a standing wave of a laser light. When molecules are trapped in a two- or three-dimensional lattice, a large number of molecules are trapped at different positions. Therefore, we can measure the spectrum with a high signal-to-noise ratio and suppress the collision shift.

For the magic trap frequencies the Stark shift of the (0,0) and (1,0) states are equal, and the transition frequency is no longer shifted by the trap laser. For a $^{174}\text{Yb}^6\text{Li}$ molecule, the magic trap frequency also exists in the far-off resonance region for all transitions. Therefore, the Stark shift is less than 10^{-16} even when the trap laser frequency is detuned from the magic trap frequency by $\sim 1 \text{ MHz}$. Thus, measuring the $^{174}\text{Yb}^6\text{Li}$ vibrational transition frequency is more advantageous for reducing the frequency uncertainty than measuring the Sr_2 vibrational transition [17], whose magic trap frequencies exist only in the quasisonant region.

The (0,0) \rightarrow (1,0) transition is observed via a Raman transition. We can also eliminate the Stark shift induced by Raman lasers by using select Raman laser frequencies. The magic Raman frequencies in the far-off resonance region are particularly useful because of their low sensitivity to the power fluctuations of the Raman lasers.

A group in Kyoto is preparing to produce $^{174}\text{Yb}^6\text{Li}$ molecules via the Feshbach resonance. They have already simultaneously trapped ^{174}Yb and ^6Li atoms and observed the quantum degenerated states [22,23]. Given the large transition dipole moment between the $X^2\Sigma$ and the $B^2\Sigma$ states (see Table I), it will be possible to force all of the $^{174}\text{Yb}^6\text{Li}$ molecules into the vibrational-rotational ground state, which Ni *et al.* and Aikawa *et al.* have done successfully with alkali-alkali molecules [24,25].

The magic trap and Raman frequencies in the far-off resonance region may also exist for other molecular vibrational frequencies (including overtone transitions) if the vibrational transition in the electronic ground state is neither the highest nor the lowest of all the electronic states. Precisely measuring the molecular vibrational transition frequencies is useful for testing of the variance in the proton-to-electron mass ratio.

- [1] E. R. Hudson, H. J. Lewandowski, B. C. Sawyer, and J. Ye, *Phys. Rev. Lett.* **96**, 143004 (2006).
- [2] E. Reinhold, R. Buning, U. Hollenstein, A. Ivanchik, P. Petitjean, and W. Ubachs, *Phys. Rev. Lett.* **96**, 151101 (2006).
- [3] V. V. Flambaum and M. G. Kozlov, *Phys. Rev. Lett.* **98**, 240801 (2007).
- [4] M. T. Murphy, V. V. Flambaum, S. Muller, and C. Henkel, *Science* **320**, 1611 (2008).
- [5] M. M. Boyd, A. D. Ludlow, S. Blatt, S. M. Foreman, T. Ido, T. Zelevinsky, and J. Ye, *Phys. Rev. Lett.* **98**, 083002 (2007).
- [6] T. Rosenband, D. B. Hume, P. O. Schmidt, C. W. Chou, A. Brusch, L. Lorini, W. H. Oskay, R. E. Drullinger, T. M. Fortier, J. E. Stalnaker, S. A. Diddams, W. C. Swann, N. R. Newbury, W. M. Itano, D. J. Wineland, and J. C. Bergquist, *Science* **319**, 1808 (2008).
- [7] A. Shelkownikov, R. J. Butcher, C. Chardonnet, and A. Amy-Klein, *Phys. Rev. Lett.* **100**, 150801 (2008).
- [8] H. L. Bethlem, M. Kajita, B. Sartakov, G. Meijer, and W. Ubachs, *Eur. Phys. J. Spec. Topics* **163**, 55 (2008).
- [9] V. V. Flambaum and M. G. Kozlov, *Phys. Rev. Lett.* **99**, 150801 (2007).
- [10] D. DeMille, S. Sainis, J. Sage, T. Bergeman, S. Kotochigova, and E. Tiesinga, *Phys. Rev. Lett.* **100**, 043202 (2008).
- [11] M. Kajita, *Phys. Rev. A* **77**, 012511 (2008).
- [12] M. Kajita, *New J. Phys.* **11**, 055010 (2009).
- [13] J. D. Weinstein, R. DeCarvalho, T. Guillet, B. Friedrich, and J. M. Doyle, *Nature* **395**, 148 (1998).
- [14] M. Kajita and Y. Moriwaki, *J. Phys. B* **42**, 154022 (2009).
- [15] M. Kajita, M. Abe, M. Hada, and Y. Moriwaki, *J. Phys. B* **44**, 025402 (2011).
- [16] T. Zelevinsky, S. Kotochigova, and J. Ye, *Phys. Rev. Lett.* **100**, 043201 (2008).
- [17] S. Kotochigova, T. Zelevinsky, and J. Ye, *Phys. Rev. A* **79**, 012504 (2009).
- [18] G. Gopakumar, M. Abe, B. P. Das, M. Hada, and K. Hirao, *J. Chem. Phys.* **133**, 124317 (2010).
- [19] T. Zanon-Willette, A. D. Ludlow, S. Blatt, M. M. Boyd, E. Arimondo, and J. Ye, *Phys. Rev. Lett.* **97**, 233001 (2006).
- [20] S. Kotochigova, *J. Chem. Phys.* **128**, 024303 (2008).
- [21] G. Gopakumar, M. Abe, M. Hada, and M. Kajita (in preparation).
- [22] M. Okano, H. Hara, M. Muramatsu, K. Doi, S. Uetake, Y. Takasu, and Y. Takahashi, *Appl. Phys. B* **98**, 691 (2010).
- [23] H. Hara, Y. Takasu, Y. Yamaoka, J. M. Doyle, and Y. Takahashi, *Phys. Rev. Lett.* **106**, 205304 (2011).
- [24] K.-K. Ni, S. Ospelkaus, M. H. G. De Miranda, A. Pe'er, B. Neyenhuis, J. J. Zierbel, S. Kotochigova, P. S. Julienne, D. S. Jin, and J. Ye, *Science* **322**, 231 (2008).
- [25] K. Aikawa, D. Akamatsu, M. Hayashi, K. Oasa, J. Kobayashi, P. Naidon, T. Kishimoto, M. Ueda, and S. Inouye, *Phys. Rev. Lett.* **105**, 203001 (2010).